while for $\Omega = K = \frac{1}{2}$,

$$\langle s_{z'}\rangle_{M=I} = (I+1)^{-1}\Big\{ \tfrac{1}{4}\sum_{nl}(2l+1)^{-1}\{ |C_{\frac{1}{2}}^{w}(l+\tfrac{1}{2})|^2$$
$$- |C_{\frac{1}{2}}^{w}(l-\tfrac{1}{2})|^2 - 4[l(l+1)]^{\frac{1}{2}}C_{\frac{1}{2}}^{w}(l+\tfrac{1}{2})$$
$$\times C_{\frac{1}{2}}^{w}(l-\tfrac{1}{2})\} - \tfrac{1}{2}w(-1)^{I+\frac{1}{2}}(I+\tfrac{1}{2})$$
$$\times \sum_{nl}(2l+1)^{-1}[l^{\frac{1}{2}}C_{\frac{1}{2}}^{w}(l-\tfrac{1}{2})$$
$$- (l+1)^{\frac{1}{2}}C_{\frac{1}{2}}^{w}(l+\tfrac{1}{2})]^2 \Big\}. \quad (C4)$$

When $I = \frac{1}{2}$, (C4) reduces to

$$\tfrac{1}{6}\sum_{nl}(2l+1)^{-1}\{ (2l+3)|C_{\frac{1}{2}}^{w}(l+\tfrac{1}{2})|^2$$
$$+ (2l-1)|C_{\frac{1}{2}}^{w}(l-\tfrac{1}{2})|^2$$
$$- 8[l(l+1)]^{\frac{1}{2}}C_{\frac{1}{2}}^{w}(l+\tfrac{1}{2})C_{\frac{1}{2}}^{w}(l-\tfrac{1}{2})\} \quad (C5)$$

for $w = 1$, and is simply equal to $-\frac{1}{6}$ when $w = -1$. In the latter case, we simply get Nilsson's result[30]

$$\mu = \tfrac{1}{3}[(g_l - g_c)a_k + g_l + g_c - \tfrac{1}{2}g_s]. \quad (C6)$$

This formula makes it possible to determine the parity of some rotational bands which have $I_0 = \frac{1}{2}$. For if one knows both μ and a_k, and finds that they are not related through (C6), one can conclude that $w = +1$. It is in this way that we have assigned even parity to the ground states of W^{183} and Tm^{169}; see Table III, footnote e.

Inelastic Scattering of Neutrons*

Ira L. Morgan

Department of Physics, University of Texas, Austin, Texas

(Received May 14, 1956)

Inelastic scattering of fast neutrons in Al, Na, S, Fe, Cu, I, and Cd has been detected by observing the gamma radiation from the excited states. The cross sections for gamma-ray production at energies well above threshold in Fe and Al have been measured. The gamma-ray energies observed correspond to known levels, transitions between levels, or de-excitation from neutron capture.

INTRODUCTION

A WELL-KNOWN method for investigating the levels in light, medium, and heavy nuclei is by the inelastic scattering of neutrons. This process involves the interaction of a neutron with the nucleus in which the de-excitation of the nucleus is by gamma-ray emission accompanied by an inelastically scattered neutron. If the level of excitation is high enough, cascade between levels may occur. Competing processes also have a direct influence on the excitation curve. Many investigators[1-4] have studied the resulting gamma radiation due to inelastically scattered neutrons. In general this has been at one energy or in the region of threshold for production of the gamma radiation. In the present investigation, the shape of the excitation curves at energies well above threshold has been obtained in order to study the effect of additional cascading from higher levels, as well as competing reactions. The energy of the gamma radiation observed in this work is consistent with known energy levels, capture processes, or cascades between levels.

EXPERIMENTAL PROCEDURE

The University of Texas Van de Graaff generator was used to produce the reactions $D(d,n)He^3$ and $Li^7(p,n)Be^7$, providing neutrons in the energy range

required. A deuterium gas cell was used which was 2 cm in depth with a 0.0001-in. Ni foil covering the entrance hole which passed the deuteron beam. The Li^7 target was evaporated on a silver backing and was found to be 35 kev thick as measured by the threshold method.

A "ring" geometry was used and found to be convenient for those elements studied, producing high intensities and a low background. Metallic Na was shaped in the form of a ring and contained in kerosene, except during periods of bombardment. Sulfur was melted and molded into a ring, while iodine in the form of crystals was packed in a thin-wall hollow Al ring. The other elements were easily machined. The attenuators, which were conical in shape, were of paraffin or
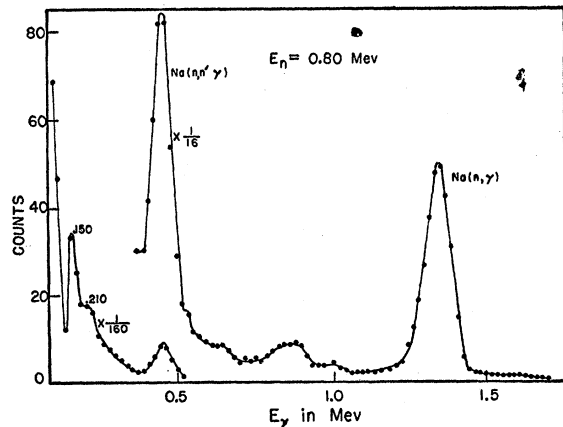

FIG. 1. Pulse-height distribution of the gamma rays produced by 800-kev neutron bombardment of Na.

[1] M. A. Rothman and C. E. Mandeville, Phys. Rev. 93, 796 (1954).
[2] R. M. Kiehn and C. Goodman, Phys. Rev. 92, 652 (1953).
[3] Scherrer, Allison, and Faust, Phys. Rev. 96, 386 (1954).
[4] J. J. Van Loef and D. A. Lind, Phys. Rev. 101, 103 (1956).
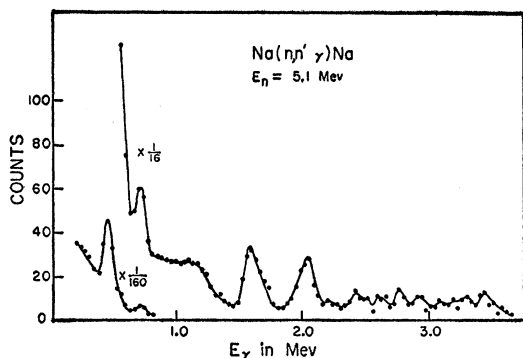
FIG. 2. Pulse-height distribution of the gamma rays produced by the inelastic scattering of 5.1-Mev neutrons in Na.

lead, depending upon the neutron energy and the amount of attenuation needed.

The spectrometer consisted of a $1\frac{1}{2}$ in.$\times 1\frac{1}{2}$ in. NaI(Tl) crystal mounted on a DuMont 6292 photomultiplier tube and the pulses were analyzed with a 20-channel pulse-height analyzer. The over-all resolution, as measured with Cs^{137} gamma rays, was maintained at approximately 8%. The target thickness and the beam current, which was integrated using a standard capacitor, provided the determination of the flux at each observation. A ZnS counter which was previously calibrated using a standard long counter was also employed as a monitor.

In obtaining the spectra from which the cross sections were calculated the following corrections were employed. The prompt background due to elastically scattered neutrons was subtracted by placing a Plexiglas (CH_2) ring in place of the scatterer. A second background, due to the long-lived activity which builds up in the detector, was subtracted. A third correction was made by subtracting out the Compton distributions of the higher energy gamma rays. Multiple neutron scattering was not considered since previous measurements
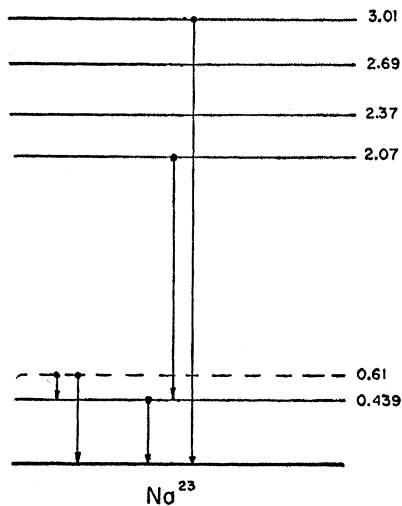

FIG. 3. Proposed transitions in Na^{23}.

at these energies lead us to believe this is negligible. Gamma-ray absorption in the rings was calculated to be less than 6% for $E_\gamma = 0.667$ Mev. All measurements were taken at 100° to the neutron beam, hence the cross sections calculated are given in barns/steradian at 100°. Isotropy is assumed for some gamma rays merely to obtain a comparison with nonelastic cross sections or calculated cross sections.

RESULTS

$Na^{23}(n,n'\gamma)Na^{23}$

A metallic Na ring was bombarded with neutrons of energies 800 kev and 5.1 Mev. The pulse-height distributions obtained are shown in Figs. 1 and 2, respectively. At $E_n = 800$ kev, six gamma rays are observed with energies of 0.150, 0.210, 0.439, 0.610, 0.870, and 1.34 Mev. The gamma rays are ascribed to the following reactions: $Na^{23}(n,n'\gamma)$—0.150, 0.439, 0.610 Mev; I^{123}-$(n,n'\gamma)$—0.210 Mev; $Na^{23}(n,\gamma)Na^{24}$—0.870, 1.34 Mev. The latter capture reaction shows a cascade gamma ray
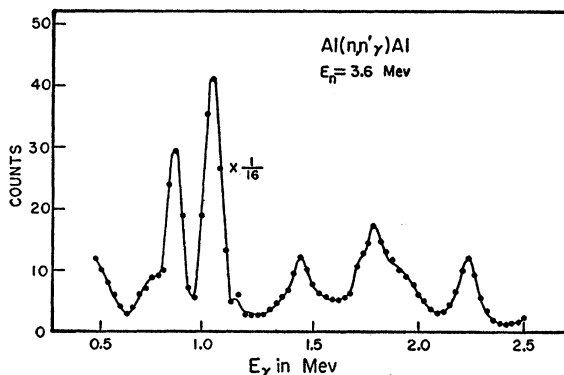

FIG. 4. Pulse-height distribution of the gamma rays produced by the inelastic scattering of 3.6-Mev neutrons in Al.

between the 1.34-Mev and 0.870-Mev levels. The 0.470-Mev gamma ray is completely obscured by the very intense 0.439-Mev gamma radiation from $Na^{23}(n,n'\gamma)N^{23}$.

At $E_n = 5.1$ Mev, four gamma rays are clearly shown in addition to several unresolved lines. The gamma-ray energies are 0.439, 0.650, 1.63, 2.07 Mev and are ascribed to the reaction $Na^{23}(n,n'\gamma)Na^{23}$. The 1.63-Mev gamma ray is ascribed to the transition between the 2.07 and 0.439 levels. The higher energy unresolved lines in $Na^{23}(n,n'\gamma)Na^{23}$ were later resolved with a 3 in.$\times 3$ in. NaI crystal and have energies consistent with known levels in Na^{23}. Figure 3 shows the proposed transitions in Na^{23} as concluded from the spectra obtained.

$Al^{27}(n,n'\gamma)Al^{27}$

The pulse-height distribution of the gamma rays resulting from the inelastic scattering of 3.6-Mev neutrons is shown in Fig. 4. Gamma rays of energies 0.85, 1.05, 1.40, 1.74, and 2.63 Mev are observed. A spectrum taken at higher energies also shows a 2.72-Mev gamma

ray. Since there are no known levels at 1.40 and 1.74 Mev, these gamma rays are attributed to cascades between the 2.63- and 0.843-Mev levels and the 2.75- and 1.01-Mev levels, respectively. There is also slight evidence of a 1.1-Mev gamma ray, possibly due to a transition between the 2.23- and 1.01-Mev levels. Figure 5 shows the proposed transitions between excited levels in Al^{27}.

The cross section for production of the 0.83- and 1.01-Mev gamma rays due to inelastic scattering in Al^{27} is shown in Fig. 6. The cross section at $100°$ to the neutron beam for the production of the 0.83-Mev and 1.01-Mev gamma rays shows an average value of 0.025 barn/steradian and 0.040 barn/steradian, respectively. The variations in the excitation curves are attributed to the competing $Al^{27}(n,p)Mg^{27}$ process which has a threshold of 2.7 Mev with resonances at 3.5, 3.75, and 4.0 Mev. The resonant values in the inelastic excitation correspond closely to the minima observed in the
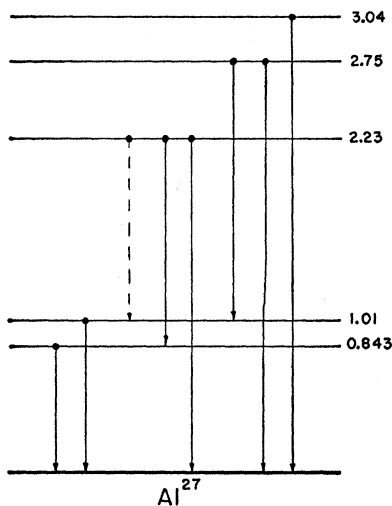

FIG. 6. Differential cross section for gamma-ray production due to inelastic scattering of neutrons in Fe and Al. △—NRL data[8]; ✕—Bartol data [Rothman, Hans, and Mandeville, Phys. Rev. 100, 83 (1955)].

FIG. 5. Proposed transitions in Al^{27}.

$Al^{27}(n,p)Mg^{27}$ excitation curve. Assuming isotropy for both gamma rays, the average values for $\sigma_{in} + \sigma_{n,p} = \sigma_c$ is 0.803 barn, which compares favorably with non-elastic cross-section measurements.[5] The value $\sigma_c = 0.610†$ barn is obtained from theoretical considerations based on the "complex potential model"[6] if it is assumed that $V_0 = 19$ Mev and $\zeta = 0.05$. These parameters were selected from elastic scattering data previously obtained. The estimated cross section for production of the 2.25 Mev gamma ray at $E_n = 3.7$ Mev is 0.056 barn/steradian at $100°$.

$S^{32}(n,n'\gamma)S^{32}$.

The inelastic scattering of 3.7-Mev neutrons from sulfur produced two gamma rays with energies of

2.20 and 0.89 Mev. Presumably the 2.20-Mev gamma ray arises from $S^{32}(n,n'\gamma)S^{32}$ and the 0.89-Mev gamma ray from $S^{33}(n,n'\gamma)S^{33}$. The calculated cross section for production of the 2.60-Mev gamma ray is 0.034 barn/steradian at $100°$. If isotropy is assumed, this value compares favorably with previous results.[7]

$Fe(n,n'\gamma)Fe$

Neutron bombardment of Fe at $E_n = 3.7$ Mev produced seven distinct gamma rays with energies of 0.84, 1.25, 1.81, 2.06, 2.57, 3.07, and 3.44 Mev. The differential cross section for production of the 0.84-Mev gamma ray has been calculated in the energy range of 3.3-Mev to 5.0-Mev neutron bombarding energy. The pulse-height distribution of the 0.84-Mev gamma ray at $E_n = 4.25$ Mev as shown in Fig. 7 is typical of the spectra obtained for the excitation. The excitation as shown in Fig. 6 shows a distinct rise at approximately 3.0 Mev with a flat tail to 5.0 Mev. This rise is attributed to cascade between the 3.07-Mev level and
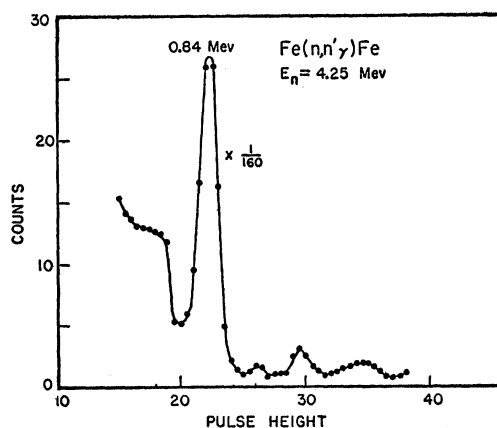
FIG. 7. Pulse-height distribution of the 0.84-Mev gamma ray produced by the inelastic scattering of 4.25-Mev neutrons in Fe.

[5] Taylor, Lönsjö, and Bonner, Phys. Rev. 100, 174 (1955).
† Note added in proof.—A value of $\sigma_c = 0.321$ barn is obtained if $V_0 = 42$ Mev and $\zeta = 0.03$.
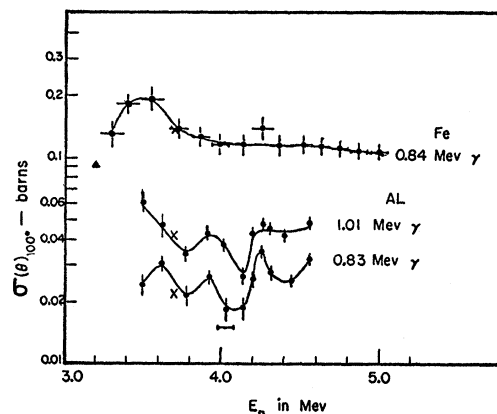[6] Feshbach, Porter, and Weisskopf, Phys. Rev. 96, 448 (1954).

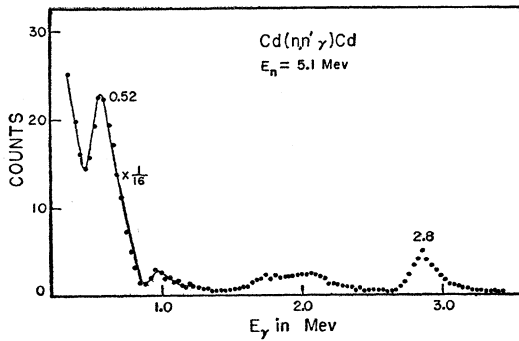[7] Grace, Beghian, Preston, and Halban, Phys. Rev. 82, 969 (L) (1951).

FIG. 8. Pulse-height distributions of the gamma rays arising from 5.1-Mev neutron bombardment of Cd.

the 0.84-Mev levels. The flat region of the excitation would indicate that the contribution of cascades from higher levels or the competition due to other reactions is probably small. Recent publications[4] have shown the 0.84-Mev gamma ray to be anisotropic, with $W(\theta) = 1 + 0.54P_2(\cos\theta) - 0.28P_4(\cos\theta)$. This result gives $\sigma_{in} = 1.36$ barns for the 0.84-Mev gamma ray at $E_n = 4.25$ Mev. σ_{in} for the 0.84-Mev gamma ray plus the contribution due to other inelastically produced gamma rays compares favorably with $\sigma_c = 1.50$ barns, the measured nonelastic cross section[5] for Fe. A calculated value of $\sigma_c = 1.53$ barns was obtained using the nuclear model previously stated. The cross sections for the production of higher energy gamma rays from Fe are calculated relative to the production of the 0.84-Mev gamma ray and are shown in Table I.

Cu $(n,n'\gamma)$Cu

Inelastic scattering at $E_n = 3.7$ Mev has produced six gamma rays with energies of 0.68, 0.97, 1.10, 1.32, 1.90, and 2.60 Mev. The inelastic excitation for the production of the 0.68- and 0.97-Mev gamma rays is in progress as well as a determination of the cross sections for production.

Cd $(n,n'\gamma)$Cd

Figure 8 shows the pulse-height distribution of the gamma rays from the inelastic scattering of 5.10-Mev neutrons in Cd. Two prominent lines appear at 0.52
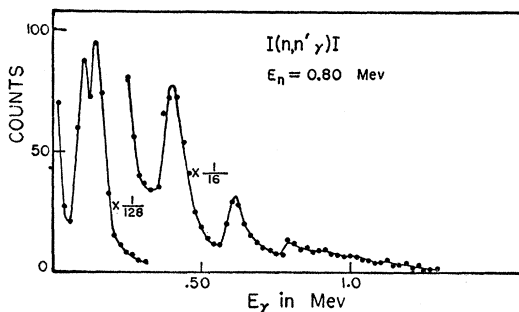

FIG. 9. Pulse-height distribution of the gamma rays produced by 800-kev neutron bombardment of I.

and 2.80 Mev. Gamma rays of higher energy were not detectable above the background.

$I^{128}(n,n'\gamma)$

Figure 9 shows the pulse-height spectrum obtained due to the inelastic scattering of 0.80-Mev neutrons in I. Five gamma rays are clearly shown and have energies of 0.134, 0.210, 0.410, 0.620, and 0.780 Mev.

TABLE I. A list of the gamma rays observed and their proposed method of production. The cross section for production of the gamma ray is shown at those energies for which it was calculated. Gamma-ray energies are given to within ±20 kev since the analyzer calibration in general provided a window width of approximately 20 kev.

Element	Gamma-ray energy (Mev)	Method of production	Cross section[a] for γ-ray production at 100° barns/steradian	Neutron bombarding energy (Mev)
Na	0.150	(n,n')	...	0.80
	0.438	(n,n')	>0.075	5.1; 0.80
	0.610	(n,n')	...	5.1; 0.80
	2.07	(n,n')	...	5.1
	1.34	(n,γ)	...	0.80
	1.58	(n,n')-cascade γ	...	5.1
	0.87	(n,γ)-cascade γ	...	0.80
Al	0.83	(n,n')	}see Fig. 6	
	1.01	(n,n')		
	1.45	(n,n')-cascade γ	...	
	1.75	(n,n')-cascade γ	...	
	2.25	(n,n')	0.056	3.6
S	0.89	(n,n') in S^{33}	...	
	2.20	(n,n') in S^{32}	0.034	3.7
Fe	0.84	(n,n')	see Fig. 6	
	1.25	(n,n')	0.024	3.7
	1.81	(n,n')	0.025	3.7
	2.06	(n,n')	0.030	3.7
	2.57	(n,n')	0.007	3.7
	3.07	(n,n')	0.014	3.7
	3.44	(n,n')	0.021	3.7
Cu	0.68	(n,n')	...	3.7
	0.97	(n,n')	...	3.7
	1.10	(n,n')	...	3.7
	1.32	(n,n')	...	3.7
	1.90	(n,n')	...	3.7
	2.60	(n,n')	...	3.7
I	0.134	(n,n')	...	0.80
	0.210	(n,n')	...	0.80
	0.420	(n,n')	...	0.80
	0.620	(n,n')	...	0.80
	0.780	(n,n')	...	0.80
Cd	0.52	(n,n')	...	5.1
	2.80	(n,n')	...	5.1

[a] The errors in these cross sections are estimated to be ±20%.

The spectrum is uncorrected and is shown as it appeared in the 20-channel analyzer. A Pb attenuator was used to shield the NaI(Tl) crystal.

ACKNOWLEDGMENTS